Journal of Molecular Liquids 216 (2016) 821–829

Contents lists available at ScienceDirect

Journal of Molecular Liquids

journal homepage: www.elsevier.com/locate/molliq

Potentiometric, thermodynamics and theoretical calculations of some rhodanine derivatives

A.Z. El-Sonbati, M.A. Diab, A.F. Shoair, A.A. El-Bindary *, A.M. Barakat

Chemistry Department, Faculty of Science, Damietta University, Damietta 34517, Egypt

ARTICLE INFO

Article history:
Received 30 October 2015
Received in revised form 14 December 2015
Accepted 17 January 2016
Available online xxxx

Keywords:
Rhodanines
Potentiometry
Thermodynamics
Hammett's constant

ABSTRACT

A series of 5-(4′-alkylphenylazo)-3-phenylamino-2-thioxothiazolidin-4-one ($\mathbf{HL_n}$) have been prepared and characterized by elemental analysis, ^{1}H NMR and IR spectra. X-ray diffraction pattern of ligand ($\mathbf{HL_2}$) was studied. The geometrical structures of these ligands are carried out by HF method with 3-21G basis set. Proton-ligand dissociation constant of ligands ($\mathbf{HL_n}$) and their metal–ligand stability constants of Mn^{2+}, Co^{2+}, Ni^{2+} and Cu^{2+} have been determined potentiometrically in 0.1 M KCl and 30% (v/v) DMSO–water mixture at 298, 308 and 318 K. The stability constants of the formed complexes increase with the order: $Mn^{2+} < Co^{2+} < Ni^{2+} < Cu^{2+}$. The effect of temperature was studied and the corresponding thermodynamic parameters (ΔG, ΔH and ΔS) were derived and discussed. The dissociation process is non-spontaneous, endothermic and entropically unfavorable. The formation of the metal complexes has been found to be spontaneous, endothermic and entropically favorable. Proton–ligand dissociation constant (pK^H) of the ligands increases according to the following order *p*-($OCH_3 > H > NO_2$) as expected from Hammett's constant (σ^R).

1. Introduction

Azo compounds based on rhodanine usually react as chelating ligands with transition metal ions by bonding through the oxygen and hydrazinic nitrogen atoms [1,2]. These compounds were synthesized as potential medicinal preparation [3] and can also be used as analytical reagents [4]. Many binary complexes of transition and inner transition metals have been studied potentiometrically [5,6]. There has been growing interest in studying azo compounds especially heterocyclic compounds and their transition metal complexes because of their wide importance in industrial fields [7] such as, dying of textile fibers [8], biological studies [9] and high technology area [10]. Metal complexes of rhodanine have been extensively studied because rhodanine possesses good synthetic flexibility, selectivity and sensitivity towards the central metal atom [11,12].

In continuation of our previous work [13–15], we report herein the dissociation constant of 5-(4′-methoxyphenylazo)-3-phenylamino-2-thioxothiazolidin −4-one ($\mathbf{HL_1}$), 5-(4′-phenylazo)-3-phenylamino-2-thioxothiazolidin-4-one ($\mathbf{HL_2}$) and 5-(4′-nitrophenylazo)-3-phenylamino-2-thioxothiazolidin-4-one ($\mathbf{HL_3}$). The stability constants of these ligand complexes with Mn^{2+}, Co^{2+}, Ni^{2+} and Cu^{2+} were measured by potentiometric studies at different temperatures. Furthermore, the corresponding thermodynamic functions of dissociation and stability constants were evaluated and discussed.

2. Experimental

2.1. Preparation of the ligands

All the compounds and solvents used are pure grade chemicals from BDH Sigma-Aldrich.

The azo dye ligands ($\mathbf{HL_n}$) were prepared previously [15] by coupling of 3-phenylamino-2-thioxothiazolidin-4-one with aniline and its *p*-derivatives (Fig. 1). A stoichiometric amount of aniline or its p-derivatives (0.01 mol) in 25 ml of hydrochloric acid (0.01 mol) was added dropwise to a solution of sodium nitrite (0.01 mol) in 20 ml of water at − 5 °C. The formed diazonium chloride was consecutively coupled with an alkaline solution of 3-phenylamino-2-thioxothiazolidin-4-one (0.01 mol) [16,17]. The colored precipitate, which was formed immediately, was filtered through a sintered glass crucible, washed several times with water and ethanol then dried in a vacuum desiccator over anhydrous $CaCl_2$.

The resulting formed ligands are:

HL_1 = 5-(4′-Methoxyphenylazo)-3-phenylamino-2-thioxothiazolidin-4-one;
HL_2 = 5-(phenylazo)-3-phenylamino-2-thioxothiazolidin-4-one; and
HL_3 = 5-(4′-nitrophenylazo)-3-phenylamino-2-thioxothiazolidin-4-one.

* Corresponding author.
E-mail address: abindary@yahoo.com (A.A. El-Bindary).

http://dx.doi.org/10.1016/j.molliq.2016.01.084
0167-7322/

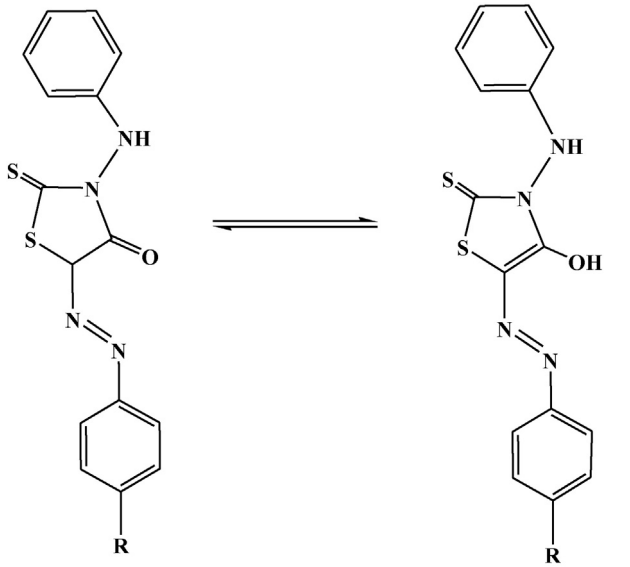

R= -OCH_3 (**HL_1**), -H (**HL_2**) and -NO_2 (HL_3)

Fig. 1. The structure of 5-(4′-alkylphenylazo)-3-phenylamino-2-thioxothiazolidin-4-one (**HL_n**).

2.2. Measurements

Elemental microanalyses of the separated ligands for C, H, and N were determined on Automatic Analyzer CHNS Vario ELIII, Germany. The ^{1}H NMR spectra was obtained by Bruker WP 300 MHz using DMSO-d_6 as a solvent containing TMS as the internal standard. IR spectra (KBr disks, 4000–400 cm^{-1}) were measured by a Jasco-4100 spectrophotometer. The pH measurements were carried out using VWR Scientific Instruments Model 8000 pH-meter accurate to ±0.01 units. The pH-meter readings in the non-aqueous medium were corrected [18]. The electrode system was calibrated according to the method of Irving et al. [19]. The temperature was controlled to within ±0.05 K by circulating thermostated water (Neslab 2 RTE 220) through the outer jacket of the vessel. X-ray diffraction analysis of the ligand powder form was recorded on X-ray diffractometer in the range of diffraction angle 2θ° = 4–70°. This analysis was carried out using CuKα radiation (λ = 1.540598 Å). The applied voltage and the tube current are 40 kV and 30 mA, respectively. The calculations of geometry optimization were performed using Perkin Elmer ChemBio 3D software by HF method with 3-21G basis set. Geometry optimization option was employed to obtain the most stable structure.

A ligand solution (0.001 M) was prepared by dissolving an accurately weighted amount of the solid in DMSO (Analar). Metal ion solutions (0.0001 M) were prepared from Analar metal chlorides in bidistilled water and standardized with EDTA [20]. Solutions of 0.001 M HCl and 1 M KCl were also prepared in bidistilled water. A carbonate-free sodium hydroxide solution in 30% (*v*/v) DMSO–water mixture was used as titrant and standardized against oxalic acid (Analar).

The apparatus, general conditions and methods of calculation were the same as in previous work [13–15]. The following mixtures (i)–(iii) were prepared and titrated potentiometrically at 298 K against standard 0.002 M NaOH in a 30% (*v*/v) DMSO–water mixture:

(i) 5 cm^3 0.001 M HCl + 5 cm^3 1 M KCl + 15 cm^3 DMSO;
(ii) 5 cm^3 0.001 M HCl + 5 cm^3 1 M KC l + 10 cm^3 DMSO + 5 cm^3 0.00 l M ligand; and
(iii) 5 cm^3 0.001 M HCl + 5 cm^3 l M KCl + 10 cm^3 DMSO + 5 cm^3 0.001 M ligand + 10 cm^3 0.0001 M metal chloride.

For each mixture, the volume was made up to 50 cm^3 with bidistilled water before the titration. These titrations were repeated for temperatures of 308 K and 318 K. The temperature was controlled to within ±0.05 K by circulating thermostated water (Neslab 2 RTE 220) through the outer jacket of the vessel. The pH measurements were carried out using VWR Scientific Instruments Model 8000 pH-meter accurate to ±0.01 units. All titrations have been carried out between pH 4.0–11.0 and under nitrogen atmosphere.

3. Results and discussion

3.1. IR spectra

The infrared spectra of ligands exhibit band at ~1230 cm^{-1}. This band can be attributed to intramolecular hydrogen-bonded-NH group, [21]. Furthermore, all ligands exhibit a strong band at 1727–1754 cm^{-1}, this is due to C═O [2]. The discussed infrared features beside the band appearing at 1435–1520 cm^{-1} can guide to assume the presence of C═N structure through resonating phenomena [22]. Such class of compounds are with different types of hydrogen bonding [23–25].

1. H-bonding of the type NH···O between the —NH (hydrazone) group and C═O group.
2. Intermolecular hydrogen bonding of the NH···O type of one molecule to another one.

The spectra of ligands do not show absorption characteristic of the N═N functions owing to the formation of the hydrazone and show no characteristic absorption assignable to NH_2 function. This confirms the formation of the azo compounds.

The strong band observed at ~1111–1123 cm^{-1} and 823–882 cm^{-1} in the ligands assigned to region may be assigned to υ(N–N) and υ(CS) vibration modes [25].

3.2. ^{1}H NMR spectra

The ^{1}H NMR spectra of all the ligands were recorded in DMSO-d_6 at room temperature using TMS as the standard. The broad signal exhibited by the ligands can be assigned to intramolecular hydrogen bonded

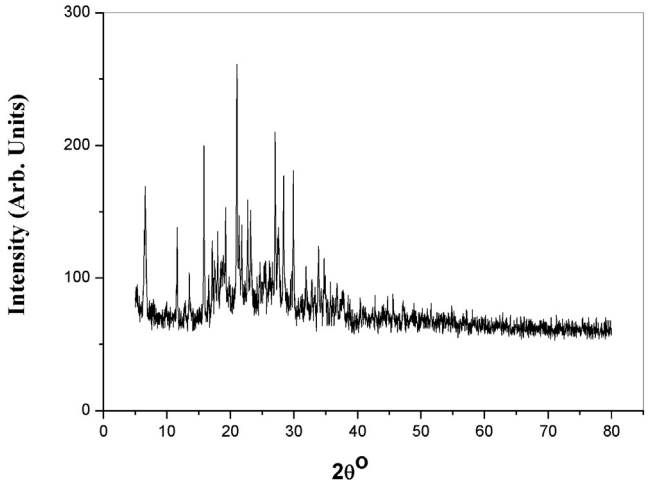

Fig. 2. XRD pattern for the ligand (**HL_2**).

proton of NH (hydrazone) at δ ~11.5 ppm and NH (3-phenylamine) at δ ~9.0 ppm was not affected by dilution and disappear in the presence of D_2O. Aromatic ring protons appear at δ ~6.5–8.0 ppm [26]. The ^{13}C NMR of ligands exhibited signals at 170–172 ppm corresponding to the carbon of (C═N) groups, signals appears at 160–163 ppm corresponding to (C═O) groups and signals around ~200 ppm corresponding to the carbon of (C═S). Ligands have different chemical shift due to aromatic ring substituent.

3.3. X-ray diffraction analysis

X-ray diffraction (XRD) pattern of ligand (**HL_2**) in powder forms is shown in Fig. 2. The XRD pattern ligand (**HL_2**) shows many peaks and this behavior indicates that the polycrystalline phase.

The XRD of (**HL_2**) shows many diffraction peaks which indicate the polycrystalline phase. The average crystallite size (ξ) can be calculated from the XRD pattern according to the Debye–Scherrer equation [27,28]:

$$\xi = \frac{K\lambda}{\beta_{1/2}\cos\theta}. \quad (1)$$

The equation uses the reference peak width at angle (θ), where λ is wavelength of X-ray radiation (1.541874 Å), *K* is constant taken as 0.95 for organic compounds [2] and $\beta_{1/2}$ is the width at half maximum of the reference diffraction peak measured in radians. The dislocation density, δ, is the number of dislocation lines per unit area of the crystal. The value

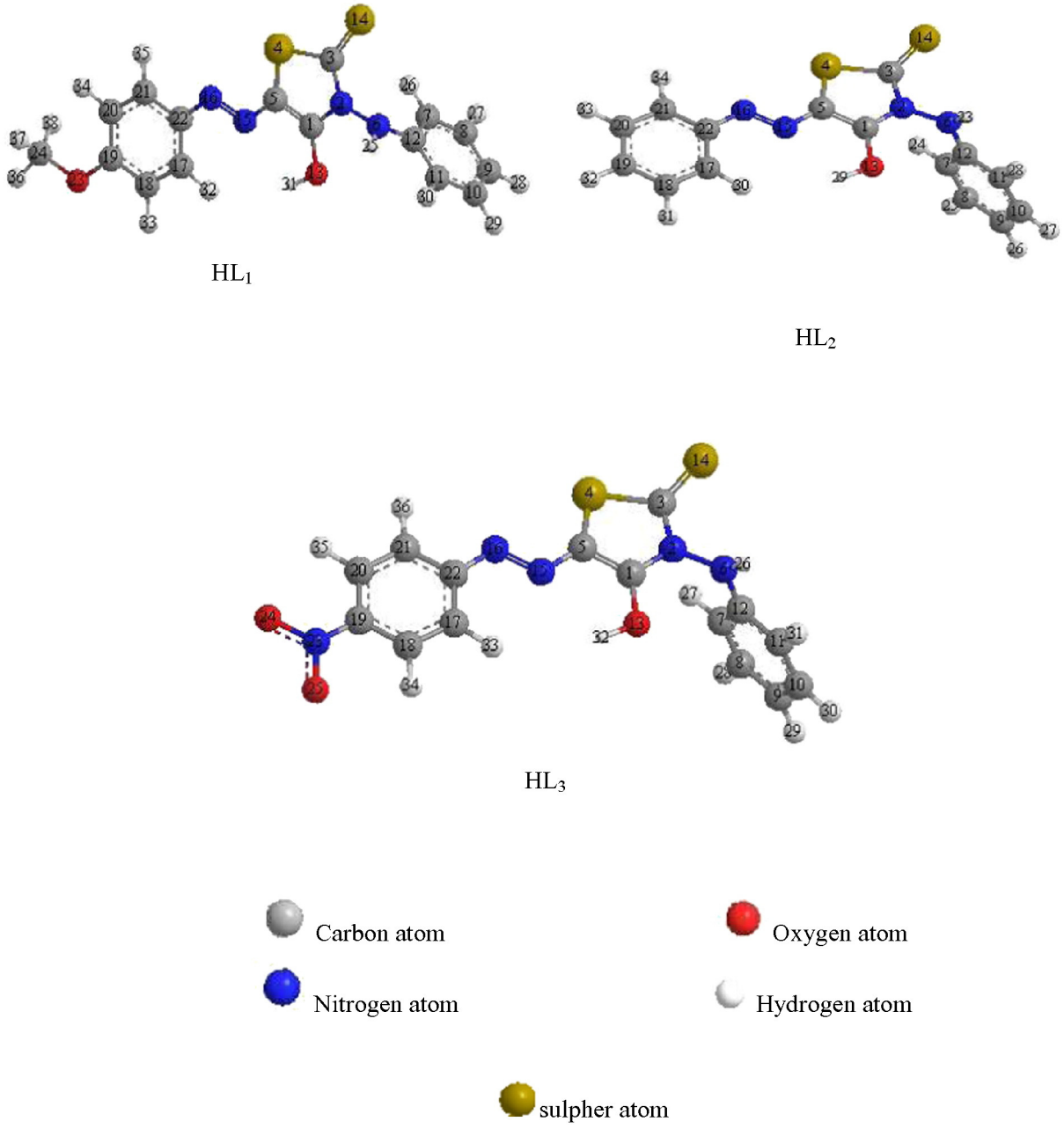

Fig. 3. The calculated molecular structures of the ligands (**HL_n**).

of δ is related to the average particle diameter (ξ) by the relation [27,28]:

$$\delta = \frac{1}{\xi^2}. \quad (2)$$

The value of ξ is calculated and found to be 76.5 nm. The value of δ is 1.71×10^{-4} nm^{-2}.

3.4. Molecular structure of the ligand

The optimized structures, bond length and bond angles of the ligands (**HL_n**) are presented in Fig. 3 and Table 1–3. The computed net charges on active centers for the ligands are found that the most negative charges in O(13), N(6) and S(14) for enol-hydrazo (Table 4). Both the highest occupied molecular orbital (HOMO) and lowest unoccupied molecular orbital (LUMO) are the main orbital that take part in chemical stability. The HOMO represents the ability to donate an electron, LUMO as an electron acceptor represents the ability to obtain an electron. The HOMO and LUMO energy for ligands calculated by HF method with 3-21G basis set is presented in Fig. 4. This electronic absorption corresponds to the transition from the ground state to the first excited state and is mainly described by one electron excitation from the highest occupied molecular orbital to the lowest unoccupied molecular orbital. Quantum chemical parameters of the ligands are obtained from calculations such as energies of the highest occupied molecular orbital (E_{HOMO}) and the lowest unoccupied molecular orbital (E_{LUMO}) as listed in Table 5. Additional parameters such as HOMO–LUMO energy gap, ΔE, absolute electronegativities, χ, chemical potentials, Pi, absolute hardness, η, absolute softness, σ, global electrophilicity, Ω, global softness, *S*, and additional electronic charge, ΔN_{max}, are calculated [29,30]. Recently, the energy gap between HOMO and LUMO has been used to prove the activity and stability of the compounds. The values of (ΔE) for **HL_1**, **HL_2**, **HL_3** ligands were found to be 0.236, 0.121 and 2.266 eV, respectively. The calculations indicated that the **HL_2** is a more stable form than the other ligands [32]. The relation between Hammett's substitution coefficients (σ^R) *vs.* energy gap (ΔE) is shown in Fig. 5.

3.5. Potentiometric studies

The average number of the protons associated with ligands (**HL_n**) at different pH values, $\overline{n}_{A,}$ was calculated from the titration curves of the acid in the absence and presence of ligands (**HL_n**).

Table 1
The selected geometric parameters for **HL_1** ligand.

Bond lengths (Å)		Bond angles (°)		Bond angles (°)	
C(24)–H(38)	1.113	H(38)–C(24)–H(37)	111.882	S(4)–C(3)–S(14)	125.048
C(24)–H(37)	1.113	H(38)–C(24)–H(36)	108.173	N(2)–C(3)–S(14)	129.265
C(24)–H(36)	1.113	H(38)–C(24)–O(23)	110.348	N(16)–N(15)–C(5)	119.236
C(21)–H(35)	1.105	H(37)–C(24)–H(36)	108.179	C(3)–S(4)–C(5)	93.394
C(20)–H(34)	1.102	H(37)–C(24)–O(23)	110.345	H(31)–O(13)–C(1)	110.086
C(18)–H(33)	1.104	H(36)–C(24)–O(23)	107.776	C(1)–N(2)–C(3)	113.994
C(17)–H(32)	1.103	C(19)–O(23)–C(24)	118.76	C(1)–N(2)–N(6)	122.379
O(13)–H(31)	0.972	H(34)–C(20)–C(21)	117	C(3)–N(2)–N(6)	123.512
C(11)–H(30)	1.104	H(34)–C(20)–C(19)	120.978	S(4)–C(5)–C(1)	110.776
C(10)–H(29)	1.103	C(21)–C(20)–C(19)	122.022	S(4)–C(5)–N(15)	131.817
C(9)–H(28)	1.103	C(20)–C(19)–C(18)	115.614	C(1)–C(5)–N(15)	117.407
C(8)–H(27)	1.103	C(20)–C(19)–O(23)	125.576	C(5)–C(1)–N(2)	116.149
C(7)–H(26)	1.103	C(18)–C(19)–O(23)	118.81	C(5)–C(1)–O(13)	123.089
N(6)–H(25)	1.051	H(33)–C(18)–C(19)	118.442	N(2)–C(1)–O(13)	120.762
C(17)–C(22)	1.346	H(33)–C(18)–C(17)	118.618	C(12)–N(6)–N(2)	123.161
C(21)–C(22)	1.346	C(19)–C(18)–C(17)	122.94	S(4)–C(3)–N(2)	105.687
C(20)–C(21)	1.343	H(35)–C(21)–C(22)	119.981		
C(19)–C(20)	1.347	H(35)–C(21)–C(20)	118.307		
C(18)–C(19)	1.347	C(22)–C(21)–C(20)	121.712		
C(17)–C(18)	1.342	H(32)–C(17)–C(22)	121.887		
C(7)–C(12)	1.345	H(32)–C(17)–C(18)	117.273		
C(11)–C(12)	1.345	C(22)–C(17)–C(18)	120.84		
C(10)–C(11)	1.342	C(17)–C(22)–C(21)	116.872		
C(9)–C(10)	1.341	C(17)–C(22)–N(16)	125.996		
C(8)–C(9)	1.341	C(21)–C(22)–N(16)	117.133		
C(7)–C(8)	1.342	C(22)–N(16)–N(15)	119.467		
C(3)–S(4)	1.789	H(29)–C(10)–C(11)	120.044		
C(5)–S(4)	1.483	H(29)–C(10)–C(9)	119.885		
C(1)–C(5)	1.356	C(11)–C(10)–C(9)	120.071		
N(2)–C(1)	1.277	H(28)–C(9)–C(10)	120.156		
C(3)–N(2)	1.268	H(28)–C(9)–C(8)	120.151		
C(22)–N(16)	1.268	C(10)–C(9)–C(8)	119.693		
N(15)–N(16)	1.252	H(27)–C(8)–C(9)	119.852		
C(12)–N(6)	1.273	H(27)–C(8)–C(7)	120.016		
N(2)–N(6)	1.356	C(9)–C(8)–C(7)	120.132		
C(19)–O(23)	1.374	H(30)–C(11)–C(12)	120.718		
C(5)–N(15)	1.268	H(30)–C(11)–C(10)	118.659		
C(3)–S(14)	1.574	C(12)–C(11)–C(10)	120.623		
C(1)–O(13)	1.365	H(26)–C(7)–C(12)	121.116		
O(23)–C(24)	1.409	H(26)–C(7)–C(8)	118.34		
		C(12)–C(7)–C(8)	120.544		
		C(7)–C(12)–C(11)	118.937		
		C(7)–C(12)–N(6)	122.902		
		C(11)–C(12)–N(6)	118.161		
		H(25)–N(6)–C(12)	114.959		
		H(25)–N(6)–N(2)	116.329		

Table 2
The selected geometric parameters for **HL_2** ligand.

Bond lengths (Å)		Bond angles (°)		Bond angles (°)	
C(21)–H(34)	1.105	H(33)–C(20)–C(21)	120.117	C(3)–N(2)–N(6)	123.504
C(20)–H(33)	1.103	H(33)–C(20)–C(19)	119.892	S(4)–C(5)–C(1)	110.761
C(19)–H(32)	1.103	C(21)–C(20)–C(19)	119.99	S(4)–C(5)–N(15)	131.837
C(18)–H(31)	1.103	H(32)–C(19)–C(20)	120.288	C(1)–C(5)–N(15)	117.402
C(17)–H(30)	1.103	H(32)–C(19)–C(18)	120.313	C(5)–C(1)–N(2)	116.162
O(13)–H(29)	0.972	C(20)–C(19)–C(18)	119.399	C(5)–C(1)–O(13)	123.084
C(11)–H(28)	1.104	H(31)–C(18)–C(19)	119.649	N(2)–C(1)–O(13)	120.753
C(10)–H(27)	1.103	H(31)–C(18)–C(17)	120.032	C(3)–S(4)–C(5)	93.403
C(9)–H(26)	1.103	C(19)–C(18)–C(17)	120.319	H(29)–O(13)–C(1)	110.072
C(8)–H(25)	1.103	H(34)–C(21)–C(22)	120.365	C(1)–N(2)–C(3)	113.989
C(7)–H(24)	1.103	H(34)–C(21)–C(20)	118.181	C(1)–N(2)–N(6)	122.383
N(6)–H(23)	1.051	C(22)–C(21)–C(20)	121.454		
C(17)–C(22)	1.348	H(30)–C(17)–C(22)	121.936		
C(21)–C(22)	1.348	H(30)–C(17)–C(18)	116.993		
C(20)–C(21)	1.342	C(22)–C(17)–C(18)	121.071		
C(19)–C(20)	1.341	C(17)–C(22)–C(21)	117.766		
C(18)–C(19)	1.341	C(17)–C(22)–N(16)	125.636		
C(17)–C(18)	1.343	C(21)–C(22)–N(16)	116.597		
C(7)–C(12)	1.345	C(22)–N(16)–N(15)	119.606		
C(11)–C(12)	1.345	H(27)–C(10)–C(11)	120.038		
C(10)–C(11)	1.342	H(27)–C(10)–C(9)	119.888		
C(9)–C(10)	1.341	C(11)–C(10)–C(9)	120.073		
C(8)–C(9)	1.341	H(26)–C(9)–C(10)	120.152		
C(7)–C(8)	1.342	H(26)–C(9)–C(8)	120.159		
C(3)–S(4)	1.789	C(10)–C(9)–C(8)	119.689		
C(5)–S(4)	1.483	H(25)–C(8)–C(9)	119.849		
C(1)–C(5)	1.356	H(25)–C(8)–C(7)	120.015		
N(2)–C(1)	1.277	C(9)–C(8)–C(7)	120.136		
C(3)–N(2)	1.267	H(28)–C(11)–C(12)	120.718		
C(22)–N(16)	1.268	H(28)–C(11)–C(10)	118.66		
N(15)–N(16)	1.252	C(12)–C(11)–C(10)	120.621		
C(12)–N(6)	1.273	H(24)–C(7)–C(12)	121.117		
N(2)–N(6)	1.356	H(24)–C(7)–C(8)	118.342		
C(5)–N(15)	1.268	C(12)–C(7)–C(8)	120.54		
C(3)–S(14)	1.574	C(7)–C(12)–C(11)	118.94		
C(1)–O(13)	1.365	C(7)–C(12)–N(6)	122.915		
		C(11)–C(12)–N(6)	118.145		
		H(23)–N(6)–C(12)	114.993		
		H(23)–N(6)–N(2)	116.379		
		C(12)–N(6)–N(2)	123.209		
		S(4)–C(3)–N(2)	105.684		
		S(4)–C(3)–S(14)	125.056		
		N(2)–C(3)–S(14)	129.26		
		N(16)–N(15)–C(5)	119.239		

Applying Eq. (3):

$$\overline{n}_A = Y \pm \frac{(V_1 - V_2)(N^\circ + E^\circ)}{(V^\circ - V_1)TC^\circ_L} \tag{3}$$

where Y is the number of available protons in ligands (**HL_n**) (Y = 1) and V_1 and V_2 are the volumes of alkali required to reach the same pH on the titration curve of hydrochloric acid and reagent, respectively, and V° is the initial volume (50 cm^3) of the mixture, TC°_L is the total concentration of the reagent, N° is the normality of sodium hydroxide solution and E° is the initial concentration of the free acid. Thus, the formation curves ($\overline{n}_A$ *vs*. pH) for the proton–ligand systems were constructed and found to extend between 0 and 1 in the $\overline{n}_A$ scale. This means that ligands (**HL_n**) have ionizable proton (the enolized hydrogen ion of the –OH group, pK^H as shown in Table 6. The completely protonated form of the ligands (**HL_n**) has dissociable proton, that dissociates in the measurable pH range. The deprotonation of the *o*-hydroxy group most probably results in the formation of stable intramolecular H– bonding with the nitrogen of the azo group. Such an interaction decreases the dissociation process of ligands (**HL_n**), i.e. increases the pK^H value [33,34].

The formation curves for the metal complexes were obtained by plotting the average number of ligands attached per metal ion ($\overline{n}_A$) *vs*. the free ligands exponent (pL). The average number of the reagent molecules attached per metal ion, $\overline{n}$, and free ligands exponent, pL, can be calculated using Eqs. (4) and (5):

$$\overline{n} = \frac{(V_3 - V_2)(N^\circ + E^\circ)}{(V^\circ - V_2)\cdot \overline{n}_A \cdot TC^\circ_M} \tag{4}$$

and

$$pL = \log_{10} \frac{\sum_{n=o}^{n=J} \beta_n^H \left(\frac{1}{[H^+]}\right)^n}{TC^\circ_L - \overline{n}\cdot TC^\circ_M} \cdot \frac{V^\circ + V_3}{V^\circ} \tag{5}$$

where TC°_M is the total concentration of the metal ion present in the solution, and $\beta^H{}_n$ is the overall proton–reagent stability constant. V_1, V_2 and V_3 are the volumes of alkali required to reach the same pH on the titration curves of hydrochloric acid, organic ligand and complex, respectively. These curves were analyzed and the successive metal–ligand stability constants were determined [35]. The values of the

Table 3
The selected geometric parameters for **HL_3** ligand.

Bond lengths (Å)		Bond angles (°)		Bond angles (°)	
C(21)–H(36)	1.105	C(19)–N(23)–O(25)	122.725	H(32)–O(13)–C(1)	110.324
C(20)–H(35)	1.104	C(19)–N(23)–O(24)	123.053	C(1)–N(2)–C(3)	113.81
C(18)–H(34)	1.104	O(25)–N(23)–O(24)	114.222	C(1)–N(2)–N(6)	122.557
C(17)–H(33)	1.103	H(35)–C(20)–C(21)	117.285	C(3)–N(2)–N(6)	123.55
O(13)–H(32)	0.971	H(35)–C(20)–C(19)	121.2	S(4)–C(5)–C(1)	110.719
C(11)–H(31)	1.104	C(21)–C(20)–C(19)	121.515	S(4)–C(5)–N(15)	132.306
C(10)–H(30)	1.103	C(20)–C(19)–C(18)	116.754	C(1)–C(5)–N(15)	116.974
C(9)–H(29)	1.103	C(20)–C(19)–N(23)	121.799	C(5)–C(1)–N(2)	116.292
C(8)–H(28)	1.103	C(18)–C(19)–N(23)	121.448	C(5)–C(1)–O(13)	123.128
C(7)–H(27)	1.103	H(34)–C(18)–C(19)	121.112	N(2)–C(1)–O(13)	120.577
N(6)–H(26)	1.051	H(34)–C(18)–C(17)	117.071	N(2)–C(3)–S(14)	129.156
C(17)–C(22)	1.347	C(19)–C(18)–C(17)	121.817	N(16)–N(15)–C(5)	119.526
C(21)–C(22)	1.346	H(36)–C(21)–C(22)	120.036	C(3)–S(4)–C(5)	93.389
C(20)–C(21)	1.343	H(36)–C(21)–C(20)	118.362		
C(19)–C(20)	1.347	C(22)–C(21)–C(20)	121.602		
C(18)–C(19)	1.347	H(33)–C(17)–C(22)	121.769		
C(17)–C(18)	1.343	H(33)–C(17)–C(18)	116.955		
C(7)–C(12)	1.345	C(22)–C(17)–C(18)	121.276		
C(11)–C(12)	1.345	C(17)–C(22)–C(21)	117.037		
C(10)–C(11)	1.342	C(17)–C(22)–N(16)	125.749		
C(9)–C(10)	1.341	C(21)–C(22)–N(16)	117.215		
C(8)–C(9)	1.341	C(22)–N(16)–N(15)	119.05		
C(7)–C(8)	1.342	H(30)–C(10)–C(11)	120.038		
C(3)–S(4)	1.789	H(30)–C(10)–C(9)	119.889		
C(5)–S(4)	1.483	C(11)–C(10)–C(9)	120.073		
C(1)–C(5)	1.356	H(29)–C(9)–C(10)	120.151		
N(2)–C(1)	1.277	H(29)–C(9)–C(8)	120.154		
C(3)–N(2)	1.267	C(10)–C(9)–C(8)	119.695		
C(22)–N(16)	1.268	H(28)–C(8)–C(9)	119.856		
N(15)–N(16)	1.252	H(28)–C(8)–C(7)	120.013		
C(12)–N(6)	1.273	C(9)–C(8)–C(7)	120.132		
N(2)–N(6)	1.356	H(31)–C(11)–C(12)	120.717		
C(19)–N(23)	1.258	H(31)–C(11)–C(10)	118.669		
C(5)–N(15)	1.267	C(12)–C(11)–C(10)	120.613		
C(3)–S(14)	1.574	H(27)–C(7)–C(12)	121.098		
C(1)–O(13)	1.365	H(27)–C(7)–C(8)	118.365		
N(23)–O(25)	1.314	C(12)–C(7)–C(8)	120.538		
N(23)–O(24)	1.314	C(7)–C(12)–C(11)	118.948		
		C(7)–C(12)–N(6)	122.855		
		C(11)–C(12)–N(6)	118.196		
		H(26)–N(6)–C(12)	114.845		
		H(26)–N(6)–N(2)	116.199		
		C(12)–N(6)–N(2)	122.928		
		S(4)–C(3)–N(2)	105.788		
		S(4)–C(3)–S(14)	125.056		

stability constants (log K_1 and log K_2) are given in Table 7. The following general remarks can be pointed out:

(i) The maximum value of $\bar{n}$ was ~2 indicating the formation of 1:1 and 1:2 (metal:ligand) complexes [36].
(ii) The metal ion solution used in the present study was very diluted (2×10^{-5} M), hence there was no possibility of formation of polynuclear complexes [37,38].
(iii) The metal titration curves were displaced to the right-hand side of the ligand titration curves along the volume axis, indicating proton release upon complex formation of the metal ion with the ligand. The large decrease in pH for the metal titration curves relative to ligand titration curves points to the formation of strong metal complexes [39].

Table 4
Net charges on active centers of the ligands (**HL_n**).

Atom	Charges		
	HL_1	HL_2	HL_3
O(13)	0.1382	0.1382	0.1382
N(6)	−0.511	−0.511	−0.511
S(14)	−0.38	−0.38	−0.38

(iv) For the same ligand at constant temperature, the stability of the chelates increases in the order: $Mn^{2+} < Co^{2+} < Ni^{2+} < Cu^{2+}$ [40,41]. This order largely reflects that the stability of Cu^{2+} complexes is considerably larger than those of other metals of the 3d series. Under the influence of both the polarizing ability of the metal ion and the ligand field [42] Cu^{2+} will receive some extra stabilization due to tetragonal distortion of octahedral symmetry in its complexes. The greater stability of Cu^{2+} complexes is produced by the well known *Jahn–Teller* effect [43].

The dissociation constant (pK^H) for ligands (**HL_n**) as well as the stability constants of their complexes with Mn^{2+}, Co^{2+}, Ni^{2+} and Cu^{2+} have been evaluated at 298, 308 and 318 K, and given in Tables 6 and 7, respectively. The enthalpy (ΔH) for the dissociation and complexation process was calculated from the slope of the plot pK^H or log *K vs.* 1/T using the graphical representation of *van't Hoff* Eqs. (6) and (7):

$$\Delta G = -2.303\, RT\, logK = \Delta H – T\Delta S \tag{6}$$

or

$$log\ K = (-\Delta H/2.303\ R)(1/T) + (\Delta S/2.303\ R). \tag{7}$$

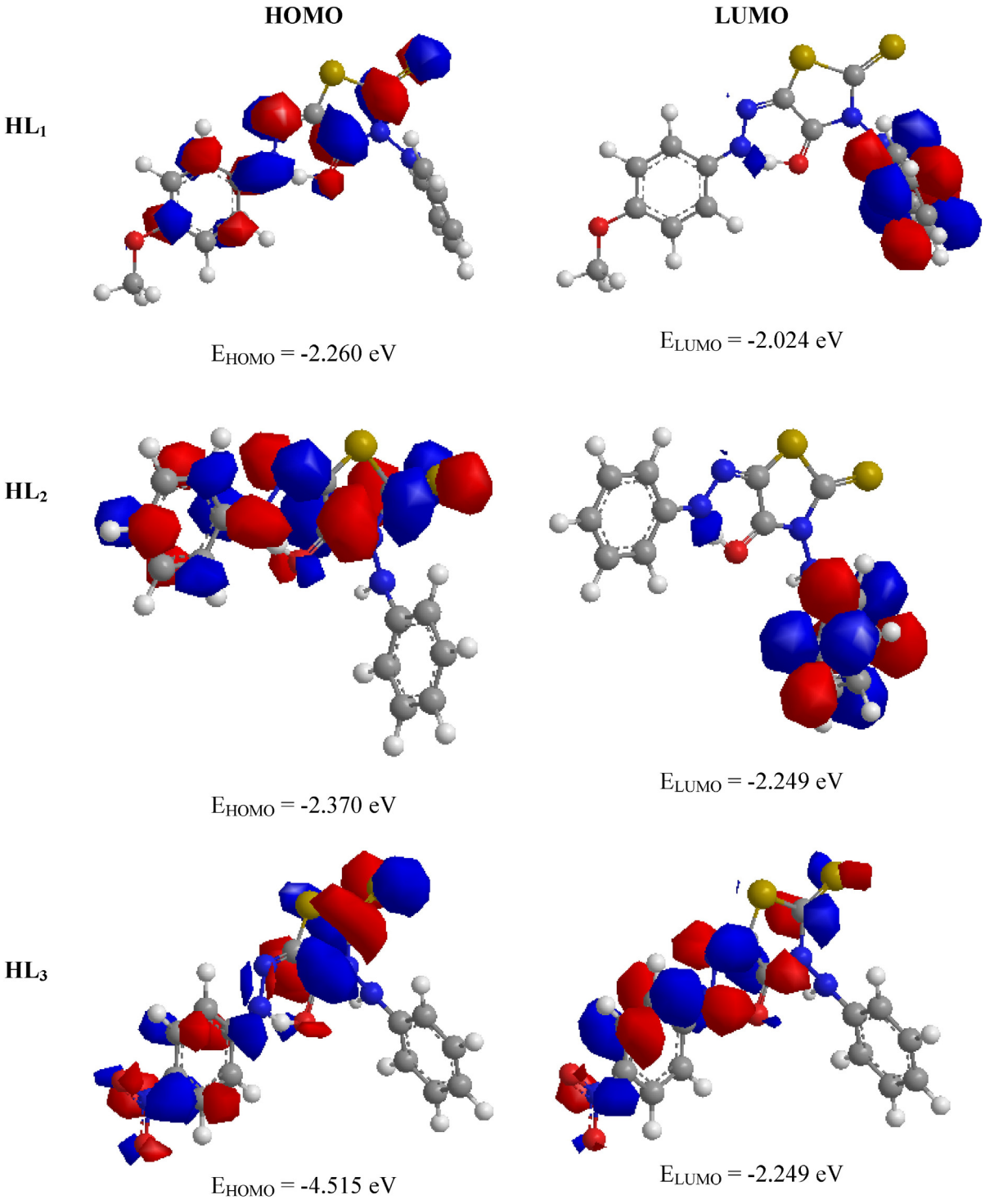

Fig. 4. The highest occupied molecular orbital (HOMO) and the lowest unoccupied molecular orbital (LUMO) of the ligands (**HL_n**).

Table 5
The calculated quantum chemical parameters for the ligands (**HL_n**).

Comp.	E_{HOMO} (eV)	E_{LUMO} (eV)	ΔE (eV)	χ (eV)	η (eV)	σ $(eV)^{-1}$	Pi (eV)	S $(eV)^{-1}$	Ω (eV)	ΔN_{max}
HL_1	−2.26	−2.024	0.236	2.142	0.118	8.475	−2.142	4.237	19.441	18.152
HL_2	−2.37	−2.249	0.121	2.309	0.060	16.529	−2.309	8.264	44.081	38.173
HL_3	−4.515	−2.249	2.266	3.382	1.133	0.883	−3.382	0.441	5.047	2.985

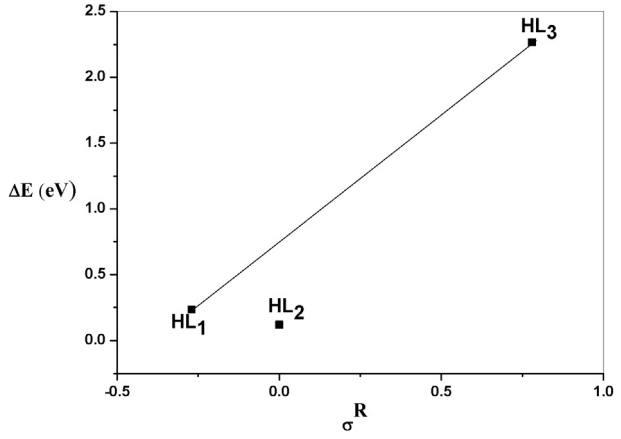

Fig. 5. The relation between Hammett's substitution coefficients (σ^R) *vs.* energy gap (ΔE) of the ligands (**HL$_n$**).

From the ΔG and ΔH values one can deduce the entropy ΔS using the well known relationships 6 and 8:

$$\Delta S = (\Delta H - \Delta G)/T. \quad (8)$$

All thermodynamic parameters of the dissociation process of ligands (**HL$_n$**) are recorded in Table 6. From these results the following conclusions can be made:

(i) The pK^H values decrease with increasing temperature, i.e. the acidity of the ligand increases [14].
(ii) A positive value of ΔH indicates that the process is endothermic.
(iii) A large positive value of ΔG indicates that the dissociation process is not spontaneous [44].
(iv) A negative value of ΔS is obtained due to the increased order as a result of the solvation process.

All the thermodynamic parameters of the stepwise stability constants of complexes are recorded in Table 8 and the obtained values of ΔH and ΔS can then be considered as the sum of two contributions: (a) release of H_2O molecules, and (b) metal–ligand bond formation. Examination of these values shows that:

(i) The stability constants ($\log K_1$ and $\log K_2$) for HLn complexes increase with increasing temperature, i.e. its stability constants increase with increasing temperature [14].
(ii) The negative value of ΔG for the complexation process suggests the spontaneous nature of such processes.

Table 6
Thermodynamic functions for the dissociation constants of ligands (**HL$_n$**) in 30% (by volume) DMSO–water mixture and 0.1 M KCl at different temperatures.

Compound	Temperature (K)	Dissociation constant	Gibbs energy kJ mol^{-1}	Enthalpy change kJ mol^{-1}	Entropy change J mol^{-1} K^{-1}
		pK^H	ΔG	ΔH	−ΔS
HL$_1$	298	8.67	49.47	27.80	72.72
	308	8.53	50.30		73.07
	318	8.37	50.96		72.84
HL$_2$	298	8.27	47.19	26.98	67.82
	308	8.11	47.83		67.70
	318	7.98	48.59		67.96
HL$_3$	298	7.88	44.96	21.79	77.77
	308	7.75	45.70		77.66
	318	7.64	46.52		77.78

Table 7
Stepwise stability constants for ML complexes of ligands (**HL$_n$**) in 30% (by volume) DMSO–water mixture and 0.1 M KCl at different temperatures.

Comp.		298 K		308 K		318 K	
	M^{n+}	$\log K_1$	$\log K_2$	$\log K_1$	$\log K_2$	$\log K_1$	$\log K_2$
HL$_1$	Mn^{2+}	6.16	4.11	6.28	4.22	6.39	4.35
	Co^{2+}	6.27	4.20	6.40	4.32	6.52	4.45
	Ni^{2+}	6.38	4.32	6.50	4.43	6.63	4.55
	Cu^{2+}	6.58	4.45	6.69	4.58	6.82	4.78
HL$_2$	Mn^{2+}	6.27	4.30	6.40	4.43	6.52	4.55
	Co^{2+}	6.40	4.41	6.53	4.52	6.66	4.65
	Ni^{2+}	6.52	4.54	6.65	4.66	6.77	4.80
	Cu^{2+}	6.73	4.63	6.85	4.75	6.99	4.88
HL$_3$	Mn^{2+}	6.49	4.52	6.61	4.64	6.74	4.75
	Co^{2+}	6.62	4.64	6.75	4.78	6.88	4.90
	Ni^{2+}	6.75	4.79	6.87	4.90	7.00	5.03
	Cu^{2+}	6.89	4.93	7.00	5.05	7.13	5.18

(iii) The ΔH values are positive, meaning that these processes are endothermic and favorable at higher temperature.
(iv) The ΔS values for the ligand complexes are positive, confirming that the complex formation is entropically favorable [13].

An inspection of the results in Table 6 reveals that the pK^H values of (**HL$_2$**) and its substituted derivatives are influenced by the inductive or mesomeric effect of the substituents. The *p*-OCH_3 derivatives

Table 8
Thermodynamic functions for the stability constants of ML complexes in 30% (by volume) DMSO–water mixture and 0.1 M KCl at 298 K.

Comp.	M^{n+}	T/K	Gibbs energy (kJ mol^{-1})		Enthalpy change (kJ mol^{-1})		Entropy change (J mol^{-1} K^{-1})	
			$-\Delta G_1$	$-\Delta G_2$	$-\Delta H_1$	$-\Delta H_2$	ΔS_1	ΔS_2
HL$_1$	Mn^{2+}	298	35.15	23.45	20.87	21.75	187.98	151.67
		308	37.04	24.89			188.00	151.41
		318	38.91	26.49			187.98	151.67
	Co^{2+}	298	35.78	23.96	37.13	22.66	196.17	156.47
		308	37.74	25.48			196.19	156.30
		318	40.67	27.10			196.17	156.47
	Ni^{2+}	298	36.40	24.65	22.66	20.85	198.21	152.68
		308	38.33	26.13			198.04	152.51
		318	40.37	27.70			198.21	152.68
	Cu^{2+}	298	37.54	25.39	21.75	29.86	198.96	185.40
		308	39.45	27.01			198.70	184.64
		318	41.53	29.10			198.97	185.42
HL$_2$	Mn^{2+}	298	35.78	24.54	22.68	22.68	196.17	158.45
		308	37.74	26.13			196.19	158.47
		318	39.70	27.70			196.17	158.45
	Co^{2+}	298	36.52	25.16	23.58	21.75	201.67	157.41
		308	38.51	26.66			201.59	157.15
		318	40.55	28.31			201.67	157.42
	Ni^{2+}	298	37.20	25.90	22.68	23.56	200.96	165.99
		308	39.22	27.48			200.97	165.72
		318	41.22	29.23			200.96	165.99
	Cu^{2+}	298	38.40	26.42	23.56	22.66	207.92	164.70
		308	40.40	28.01			207.65	164.53
		318	42.56	29.71			207.93	164.71
HL$_3$	Mn^{2+}	298	37.03	25.79	22.66	20.87	200.32	156.57
		308	38.98	27.36			200.14	156.60
		318	41.04	28.92			200.32	156.57
	Co^{2+}	298	37.77	26.48	23.58	23.60	205.88	168.04
		308	39.81	28.19			205.80	168.14
		318	41.89	29.84			205.88	168.03
	Ni^{2+}	298	38.51	27.33	22.66	21.75	205.29	164.69
		308	40.51	28.90			205.12	164.43
		318	42.62	30.63			205.30	164.69
	Cu^{2+}	298	39.31	28.13	21.75	22.66	204.90	170.45
		308	41.28	29.78			204.63	170.27
		318	43.41	31.54			204.90	170.45

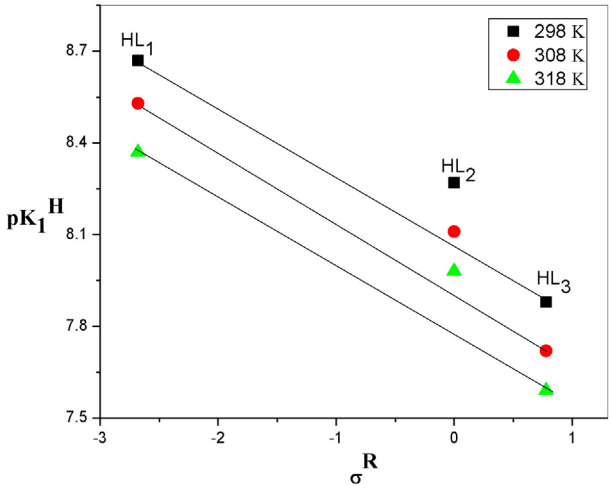

Fig. 6. Correlation of pK^H with Hammett's constant (σ^R) at 289, 308 and 310 K.

(**HL_1**) have a lower acidic character (higher pK^H values) than the *p*-NO_2 (**HL_3**). This is quite reasonable because the presence of *p*-OCH_3 group (i.e. an electron-donating effect) will enhance the electron density by their high positive inductive or mesomeric effect, whereby a stronger O–H bond is formed. The presence of *p*-NO_2 group (i.e. an electron-withdrawing effect) will lead to the opposite effect. The results are also in accordance with Hammett's *para* substituent constant values σ^R as shown in Fig. 6. Straight lines are obtained on plotting pK^H values at different temperature versus σ^R. The para substituents in the phenyl moiety have a direct influence on the pK^H values of the investigated compounds affording a maximum resonance via the delocalization of its π-system.

4. Conclusion

5-(4′-Alkylphenylazo)-3-phenylamino-2-thioxothiazolidin-4-one (**HL_n**) have been prepared and characterized by different spectroscopic techniques. The proton–ligand dissociation constants of ligands (**HL_n**) and metal–ligand stability constants of their complexes with the metal ions (Mn^{2+}, Co^{2+}, Ni^{2+} and Cu^{2+}) have been determined potentiometrically at different temperatures. The geometrical structures of these ligands are carried out by HF method with 3-21G basis set. The dissociation process is non-spontaneous, endothermic and entropically unfavorable. The pK^H value of the ligands decreases in the order **HL_1** > **HL_2** > **HL_3** as expected from Hammett's constant (σ^R). The stability constants of the formed complexes increases with increasing temperature and in the order: $Mn^{2+} < Co^{2+} < Ni^{2+} < Cu^{2+}$. The formation of the metal complexes has been found to be spontaneous, endothermic and entropically favorable. The values of (ΔE) for HL_1, HL_2, and HL_3 ligands were found to be 0.236, 0.121 and 2.266 eV, respectively. These calculations indicated that the HL_2 is more stable than the other ligands.

References

[1] A.Z. El-Sonbati, A.A. Bindary, E.M. Mabrouk, R.M. Ahmed, Spectrochim. Acta A 57 (2001) 1751–1757.
[2] A. El-Dissouky, A.A. El-Bindary, A.Z. El-Sonbati, A.S. Hilali, Spectrochim. Acta A 57 (2001) 1163–1170.
[3] F.C. Brown, C.K. Brandsher, M. Tetenbaum, P. Wilder, J. Am. Chem. Soc. 78 (1956) 384–390.
[4] W.I. Stephen, A. Townshend, Anal. Chim. Acta 33 (1965) 257–265.
[5] S.L. Johnson, L.H. Chen, R. Harbach, M. Sabet, A. Savinov, N.J.H. Cotton, A. Strongin, D. Guiney, M. Pellecchia, Chem. Biol. Drug Des. 71 (2) (2008) 131–139.
[6] A.Z. El-Sonbati, A.A.M. Belal, M.S. El-Gharib, Sh.M. Morgan, Spectrochim. Acta A 95 (2012) 627–636.
[7] M.S. Aziz, A.Z. El-Sonbati, A.S. Hilali, Chem. Pap. 56 (2002) 305–308.
[8] H. KCaokutgen, S. Ozkinali, Dyes Pigments 63 (2004) 83–88.
[9] A.Z. El-Sonbati, M.A. Diab, A.A. El-Bindary, H.A. Seyam, Spectrochim. Acta A 104 (2013) 213–221.
[10] H. Bock, K. Wittle, M. Veit, N. Wiberg, J. Am. Chem. Soc. 98 (1976) 109–120.
[11] A.Z. El-Sonbati, M.A. Diab, A.A. El-Bindary, Sh.M. Morgan, Spectrochim. Acta A 127 (2014) 310–328.
[12] A.Z. El-Sonbati, A.F. Shoair, A.A. El-Bindary, M.A. Diab, A.S. Mohamed, J. Mol. Liq. 209 (2015) 635–647.
[13] A.A. El-Bindary, M.A. Hussein, R.A. El-Boz, J. Mol. Liq. 211 (2015) 256–267.
[14] A.Z. El-Sonbati, G.G. Mohamed, A.A. El-Bindary, W.M.I. Hassan, A.K. Elkholy, J. Mol. Liq. 209 (2015) 625–634.
[15] A.A. Al-Sarawy, A.A. El-Bindary, D.N. El-Sonbati, Spectrochim. Acta A 61 (2005) 1847–1851.
[16] A.Z. El-Sonbati, I.M. El-Deen, M.A. El-Bindary, J. Mol. Liq. 215 (2016) 612–624.
[17] A.Z. El-Sonbati, M.A. Diab, A.A. El-Bindary, Sh.M. Morgan, Inorg. Chim. Acta 404 (2013) 175–187.
[18] R.G. Bates, M. Paabo, R.A. Robinson, J. Phys. Chem. 67 (1963) 1833–1838.
[19] H.M. Irving, M.G. Miles, L.D. Pettit, Anal. Chim. Acta 38 (1967) 475–488.
[20] G.H. Jeffery, J. Bassett, J. Mendham, R.C. Deney, Vogel's Textbook of Quantitative Chemical Analysis, fifth ed. Longman, London, 1989.
[21] A.Z. El-Sonbati, A.A. El-Bindary, A.A. El-Sarawy, Spectrochim. Acta A 58 (2015) 2771–2778.
[22] A. El-Dissouky, A.Z. El-Sonbati, Transit. Met. Chem. 12 (1987) 14–18.
[23] A.A. El-Bindary, A.Z. El-Sonbati, Pol. J. Chem. 74 (2000) 621–630.
[24] A.A. El-Bindary, A.Z. El-Sonbati, A. El-Dissouky, A.S. Hilali, Spectrochim. Acta A 58 (2002) 1411–1424.
[25] M. Mohan, P. Sharma, N.K. Jho, Inorg. Chim. Acta 106 (1985) 117–247.
[26] N.A. El-Ghamaz, A.Z. El-Sonbati, Sh.M. Morgan, J. Mol. Struc. 1027 (2012) 92–98.
[27] A.Z. El-Sonbati, M.A. Diab, A.A. El-Bindary, G.G. Mohamed, Sh.M. Morgan, Inorg. Chim. Acta 430 (2015) 96–107.
[28] A.A. El-Bindary, A.Z. El-Sonbati, M.A. Diab, Sh.M. Morgan, J. Mol. Liq. 201 (2015) 36–42.
[29] N.A. El-Ghamaz, A.Z. El-Sonbati, M.A. Diab, A.A. El-Bindary, G.G. Mohamed, Sh.M. Morgan, Spectrochim. Acta A 147 (2015) 200–211.
[30] A.Z. El-Sonbati, M.A. Diab, A.A. El-Bindary, A.M. Eldesoky, Sh.M. Morgan, Spectrochim. Acta A 135 (2015) 774–791.
[32] N.A. El-Ghamaz, A.Z. El-Sonbati, M.A. Diab, A.A. El-Bindary, M.K. Awad, Sh.M. Morgan, Mater. Sci. Semicond. Process. 19 (2014) 150–162.
[33] E. Farkas, H. Csoka, J. Inorg. Biochem. 89 (2002) 219–226.
[34] M.M. Omar, G.G. Mohamed, Spectrochim. Acta A 61 (2005) 929–936.
[35] M.T. Beck, I. Nagybal, Chemistry of Complex Equilibrium, Wiley, New York, 1990.
[36] M.M. Khalil, A.M. Radalla, A.G. Mohamed, Eng. Data 54 (2009) 3261–3272.
[37] P. Sanyal, G.P. Sengupta, J. Ind. Chem. Soc. 67 (1990) 342–344.
[38] S. Sridhar, P. Kulanthaip, P. Thillaiarasu, V. Thanikachalam, G.J. Manikandan, World J. Chem. 4 (2009) 133–140.
[39] V.D. Athawale, V.J. Lele, Chem. Eng. Data 41 (1996) 1015–1019.
[40] G.A. Ibañez, G.M. Escandar, Polyhedron 17 (1998) 4433–4441.
[41] G.G. Mohamed, M.M. Omar, A. Ibrahim, Eur. J. Med. Chem. 44 (2009) 4801–4812.
[42] F.R. Harlly, R.M. Burgess, R.M. Alcock, Solution Equilibria, Ellis Harwood, Chichester, 1980 257.
[43] L.E. Orgel, An Introduction to Transition Metal Chemistry Ligand Field Theory, Methuen, London, 1966 55.
[44] A. Bebot-Bringaud, C. Dange, N. Fauconnier, C. Gerard, J. Inorg. Biochem. 75 (1999) 71–78.